International Journal of Psychophysiology 183 (2023) 159–170

Contents lists available at ScienceDirect

International Journal of Psychophysiology

journal homepage: www.elsevier.com/locate/ijpsycho

Neural responding during uncertain threat anticipation in pediatric anxiety

Kalina J. Michalska [a,*], Brenda Benson [b], Elizabeth J. Ivie [c], Jessica F. Sachs [d], Simone P. Haller [b], Rany Abend [b], Daniel R. McFarlin [e], Jennifer Urbano Blackford [f,g], Daniel S. Pine [b]

[a] Department of Psychology, University of California Riverside, Riverside, CA, USA
[b] Emotion and Development Branch, National Institute of Mental Health, National Institutes of Health, Bethesda, MD, USA
[c] Department of Psychology, University of Oregon, Eugene, OR, USA
[d] Medical College of Wisconsin, Wauwatosa, WI, USA
[e] Department of Psychiatry, University of Wisconsin, Madison, WI, USA
[f] Department of Psychiatry and Behavioral Sciences, Vanderbilt University Medical Center, Nashville, TN, USA
[g] Munroe-Meyer Institute, University of Nebraska Medical Center, Omaha, NE, USA

ARTICLE INFO

Keywords:
Threat anticipation
Threat uncertainty
Pediatric anxiety
Reliability
Fmri

ABSTRACT

Excessive fear responses to uncertain threat are a key feature of anxiety disorders (ADs), though most mechanistic work considers adults. As ADs onset in childhood and confer risk for later psychopathology, we sought to identify conditions of uncertain threat that distinguish 8–17-year-old youth with AD ($n = 19$) from those without AD ($n = 33$), and assess test-retest reliability of such responses in a companion sample of healthy adults across three sites (n = 19). In an adapted uncertainty of threat paradigm, visual cues parametrically signaled threat of aversive stimuli (fear faces) in 25 % increments (0 %, 25 %, 50 %, 100 %), while participants underwent functional magnetic resonance imaging (fMRI). We compared neural response elicited by cues signaling different degrees of probability regarding the subsequent delivery of fear faces. Overall, youth displayed greater engagement of bilateral inferior parietal cortex, fusiform gyrus, and lingual gyrus during uncertain threat anticipation in general. Relative to healthy youth, AD youth exhibited greater activation in ventrolateral prefrontal cortex (vlPFC)/BA47 during uncertain threat anticipation in general. Further, AD differed from healthy youth in scaling of ventral striatum/sgACC activation with threat probability and attenuated flexibility of responding during parametric uncertain threat. Complementing these results, significant, albeit modest, cross-site test-retest reliability in these regions was observed in an independent sample of healthy adults. While preliminary due to a small sample size, these findings suggest that during uncertainty of threat, AD youth engage vlPFC regions known to be involved in fear regulation, response inhibition, and cognitive control. Findings highlight the potential of isolating neural correlates of threat anticipation to guide treatment development and translational work in youth.

1. Introduction

Anticipation of uncertain threat evokes excessive fear responses in individuals with anxiety disorders (AD) (Grupe and Nitschke, 2013). AD develop in youth and confer high risk for later psychopathology (Kessler et al., 2008), but most mechanistic work on anticipatory threat responses examines adult (see Grillon, 2008 for a review) rather than pediatric AD (e.g., Williams et al., 2015), complicating inferences. Moreover, prior studies infrequently assess test-retest reliability of anticipatory neural responding. The current study utilizes a novel threat-anticipation paradigm to compare neural responding to uncertain threat between youth with and without AD, and assess reliability of such responses.

Threat anticipation facilitates the execution of defensive responding, reflecting an adaptive process observed across species (Adolphs, 2013; Barlow, 2004; Grillon, 2008; LeDoux and Pine, 2016). However, excessive anticipatory responses constitute a key feature of clinical anxiety (DSM-5, American Psychiatric Association, 2013). To examine pathological mechanisms, anticipatory threat responsivity has been experimentally studied during expectation of aversive stimuli. Human and rodent studies show anxiety-related increases in autonomic and neural responses during anticipation of aversive stimuli, especially when

* Corresponding author at: Department of Psychology, University of California, Riverside, 900 University Ave., Riverside, CA 92521, USA.
E-mail address: kalina.michalska@ucr.edu (K.J. Michalska).

https://doi.org/10.1016/j.ijpsycho.2022.07.006
Received 12 March 2022; Received in revised form 21 June 2022; Accepted 18 July 2022
Available online 18 August 2022

such stimuli are uncertain (Chin et al., 2016; Davis et al., 2010; Grillon et al., 2008; Gorka et al., 2017), establishing preliminary links to phenotypic presentation of anxiety. The literature distinguishes between different parameters of uncertainty, including *ambiguity* and *risk* (Wu et al., 2021). Ambiguity occurs when information is unknown thus making it difficult to estimate possible outcomes (Morriss et al., 2022a, 2022b). Risk (or irreducible uncertainty), on the other hand, occurs when there is known uncertainty related to potential outcomes (Kobayashi and Hsu, 2017; Morriss et al., 2022a, 2022b; Payzan-LeNestour and Bossaerts, 2011). Here, we instruct participants about the probability of aversive outcomes in advance thereby focusing on the risk parameter. Isolating the neural correlates of threat anticipation is critical as heightened anticipation of future danger has long been viewed as a key aspect of anxiety, particularly in adolescence (Davis et al., 2010; Grupe and Nitschke, 2013). Characteristic of the adolescent period is the escalation of both sensation seeking and anxiety. Even though adolescents tend to be more sensitive to uncertainty during threat extinction and risky decision-making than either children or adults (Ganella et al., 2018; Kim et al., 2009; Linton and Levita, 2021; Morriss et al., 2019a; Pattwell et al., 2012, though see Glenn et al., 2021), they tend to be more tolerant of it as well (see Baker and Galván, 2020 for a review). It has been posited that the same aspect of risk that is rewarding for healthy adolescents—the inherent uncertainty of the outcome—may be appraised as particularly threatening in anxious adolescents (Baker and Galván, 2020). Emerging studies report a role of heightened sensitivity to uncertainty in pediatric AD, suggesting interaction of uncertainty and threat processing in this population (Nelson and Hajcak, 2017; Schmitz et al., 2011). Such insight is of particular importance since AD typically emerges in youth and precedes additional, compounding psychopathology (Beesdo et al., 2009; Kessler et al., 2005, 2008); studying youth specifically with AD enables a tighter link of observed effects to anxiety. This work suggests that youth may be particularly sensitive to variations in threat uncertainty and exhibit heightened anticipatory responding.

Research in AD frequently treats the uncertainty of experiencing the anticipated aversive stimulus as a binary property, typically contrasting conditions of uncertain (50 %) *vs* certain (100 %) threat. However, everyday situations vary continuously on threat probabilities, both with regards to timing/temporal uncertainty (not knowing when an aversive outcome may occur) (Hur et al., 2020; Radoman et al., 2021; Somerville et al., 2013), and outcome probability, (whether an aversive outcome may occur) (Hiser et al., 2021; Krain et al., 2008; Lagattuta and Sayfan, 2011). Available data (Barlow, 2000; Palitz et al., 2019) suggest that anxious individuals manifest excessive cognitive and behavioral responses based on the probability of threat in the environment. To increase the ecological value of mechanistic research on uncertain threat anticipation in pediatric anxiety, the current study extends previous work (Williams et al., 2015) via parametrically varying threat probability using cues signaling different degrees of probability about the upcoming threat.

Identifying neural mechanisms of threat uncertainty processing in pediatric AD can help guide treatment development and translational work. A variety of aversive stimuli have been employed in research, among them negative pictures which act as powerful, survival-relevant social threat cues (Glenn et al., 2021; Öhman and Mineka, 2001; Morris et al., 1998). Functional magnetic resonance imaging (fMRI) paradigms in anxious adults have revealed a network of brain regions engaged during anticipation of viewing negative pictures. For example, studies have shown that anxious versus non-anxious adults exhibit heightened amygdala, anterior insula, and orbitofrontal cortex (OFC) activity (Morriss et al., 2019a, 2019b; Sarinopoulos et al., 2010; Schienle et al., 2010; Shankman et al., 2014). Other relevant work shows greater recruitment of prefrontal cortical regions, including dorsal and medial prefrontal cortex (Morriss et al., 2021a). Lesion studies additionally suggest that ventrolateral prefrontal cortex plays a role in regulatory adaptations to uncertainty (FeldmanHall et al., 2019). The limited available data in youth with AD suggest elevated responses to uncertain anticipation in amygdala, anterior insula, and OFC (Krain et al., 2008; Williams et al., 2015), although no studies to date have parametrically modulated upcoming threat probability in pediatric AD.

The present fMRI study used an event-related threat uncertainty task adapted from Williams et al. (2015), where youth view a color bar signaling the subsequent presentation of either fearful or neutral faces. Building on this task, we parametrically varied threat probability using cues predicting the occurrence of the aversive stimuli (0 %, 25 %, 50 %, 75 %, or 100 %). Our design allowed us to simultaneously model three interconnected facets of threat anticipation that could manifest in AD: response to (1) threat *uncertainty* (as overall response to 25 %, 50 %, and 75 % and as a quadratic function with maximum uncertainty at 50 %, and intermediate uncertainty at 25 % and 75 %), (2) safety/threat *certainty* (as overall response to 0 % and 100 %), and (3) threat *probability* (as overall response to 25 %, 50 %, 75 %, and 100 % and as a linear function between 25 % and 100 %). First, we examined overall responses across the three cue types (i.e., modeled as a constant term across each cue type). Second, we examined modulated responses as a function of escalating uncertainty and threat probability cues. Of note, because this is the first study using this version of the task, we report a preliminary test of hypotheses, based in a small sample. Specifically, we hypothesized that AD youth would exhibit greater responses in amygdala, anterior insula, and OFC during uncertain threat anticipation relative to healthy youth, as well as greater modulation in these regions with increasing levels of uncertainty. Modeling neural response to uncertainty, neural response to certainty, *and* neural response to threat probability allowed us to identify which pattern of responses distinguished between youth with and without AD. As pediatric neuroimaging paradigms have rarely varied uncertainty at this level of specificity, we report findings across the entire sample as well as between AD and healthy youth.

Improved task reliability is likely to accelerate discoveries in the etiology and treatment of pediatric ADs. Meta-analytic work demonstrates that test-retest reliability of commonly used fMRI task contrasts is often relatively poor (e.g., intra-class correlation coefficient [ICC] < 0.4) in both adults (Elliott et al., 2020) and youth (Koolschijn et al., 2011). Because this is the first study using a novel task adaptation, we also examined the reliability of anticipatory neural responding. To do so, we included a companion sample of nineteen healthy adults who participated in identical study procedures at repeated visits by travelling across three sites. Including test-retest reliability may improve identification of clinically relevant targets by localizing group findings to reliable regions (see Smith et al., 2020 for a similar approach).

2. Method

2.1. Procedure

All procedures were approved by the National Institute of Mental Health institutional review board. Parents and participants provided written consent/assent. All participants were paid for their participation. Exclusion criteria were current or recent use of psychoactive medications; current suicidal ideation; lifetime history of mania, psychosis, or pervasive developmental disorder; current diagnosis of Tourette's disorder, obsessive compulsive disorder, post-traumatic stress disorder, or conduct disorder; current diagnosis of attention deficit hyperactivity disorder of sufficient severity to require pharmacotherapy; pregnancy; serious medical problems; or IQ <70. All participants underwent a semi-structured clinical interview with a trained clinical psychologist (Schedule for Affective Disorders and Schizophrenia for School-Age Children-Present and Lifetime version, K-SADS-PL; Kaufman et al., 1997) to ascertain current or past DSM-5 disorders. Participants who met DSM-5 criteria for an AD also received standard cognitive-behavioral therapy treatment following their participation. All participants and their parents completed the Screen for Child Anxiety Related Emotional Disorders (SCARED) (Birmaher et al., 1997) to assess current

Table 1
Participant demographics.

	dAnx (n = 19)	HV (*n* = 33)	Test statistic
Demographics			
Age, y			
Mean	10.63	12.43	−2.805**
SD	1.57	2.51	
Sex			
Female (%)	14 (73.68)	18 (54.55)	$\chi^2(2) = 1.87$
Male (%)	5 (26.32)	15 (45.45)	
SCARED — child			
Mean	21.72	9.83	4.318***
SD	11.06	8.47	
SCARED — parent			
Mean	29.88	5.34	8.271***
SD	13.59	7.43	
SCARED — average			
Mean	25.80	7.28	9.084***
SD	8.70	5.98	
Additional demographics			
IQ			
Mean	115.74	111.55	1.053
SD	15.64	12.30	
Race			
White (%)	11 (57.89)	13 (39.39)	
African American (%)	2 (10.53)	13 (39.39)	
Asian (%)	1 (5.26)	3 (9.09)	
Native Hawaiian and other Pacific Islander (%)	1 (5.26)	0	
Multiple race (%)	4 (21.05)	3 (9.09)	
Unknown (%)	0	1 (3.03)	
Combined family income			
<$24,999 (%)	2 (10.53)	5 (15.15)	
$25,000–$59,999 (%)	1 (5.26)	1 (3.03)	
$60,000–$89,999 (%)	4 (21.05)	3 (9.09)	
$90,000–$179,999 (%)	4 (21.05)	14 (42.42)	
>$180,000 (%)	8 (42.11)	8 (24.24)	
Unknown/missing	0	2 (6.06)	
Highest level of education (household)			
<High school (%)	1 (5.26)	1 (3.03)	
Partial college (%)	0	10 (30.30)	
4-Year college (%)	6 (31.58)	5 (15.15)	
Graduate/professional (%)	12 (63.16)	16 (3.03)	
Other/unknown (%)	0	1 (3.03)	
Anxiety diagnoses			
Generalized anxiety			
n (%)	15 (78.95)	0	
Social anxiety			
n (%)	10 (52.63)	0	
Separation anxiety			
n (%)	14 (73.68)	0	
Specific phobia			
n (%)	7 (36.84)	0	
Panic disorder			
n (%)	0	0	

Note: SCARED = Screen for Child Anxiety Related Emotional Disorders.
** $p < .01$.
*** $p < .001$.

anxiety severity.

2.2. Participants

Fifty-six participants were recruited for the present study. Following participation, 4 participants were excluded based on unusable fMRI data due to excessive motion, leaving 52 participants 8–17 years of age (M = 11.77, SD = 2.36) for the analyses. At the time of the scan, 19 of 52 participants met DSM-5 criteria for a current anxiety disorder. Of the youth who were diagnosed with an anxiety disorder, 15 (79 %) were diagnosed with Generalized Anxiety Disorder, 10 (53 %) were diagnosed with Social Anxiety Disorder, 14 (74 %) were diagnosed with Separation Anxiety, and 7 (37 %) were diagnosed with Specific Phobia (for full demographics, see Table 1).

2.3. Task

Participants completed a modified threat anticipation task based on Williams et al. (2015) while undergoing functional magnetic resonance imaging (fMRI) (Fig. 1). Participants completed three 6.4-minute runs of the task, each of which included 20 trials. On each trial participants viewed an anticipatory warning cue – a vertical bar - presented for 2 s, followed by a blank screen to produce a jittered inter-stimulus interval (4–6 s), and a set of either five threat-related (fear) or five neutral faces presented for 1 s each. The cues signaled the probability that the set of 5 fear faces will be presented, allowing us to model the likelihood of threat at incrementally varying levels. *Threat anticipation* was defined as the variable likelihoods of seeing fearful faces, signifying the level of preparation for encountering the aversive stimuli. Specifically, 5 cue types indicated varying levels of probability to see the set of fear faces (i.e., 0 %, 25 %, 50 %, 75 %, 100 % likely to see a group of 5 fear faces). Each of the 5 cues were presented 4 times in each of the three runs and counterbalanced across runs. 100 % cues (full bars) were always followed by fear faces, 75 % cues were 75 % likely to be followed by fear faces, 50 % cues (half-full bars) were equally likely to be followed by fear or neutral faces, 25 % cues were followed by fear faces 25 % of the time, and 0 % cues (empty bars) were always followed by neutral faces. During training and instructions slides at the start of the task, each cue was presented with accompanying text indicating the likelihood of seeing fear faces. Responses to fear faces were additionally modeled (see Supplemental Material for details).

As in Williams et al. (2015), pairs of neutral and fearful faces were taken from two standardized sets of facial affect (Ekman and Friesen, 2006; Tottenham et al., 2009), and participants viewed both the fear and neutral expressions for each face. To promote attention to task trials, 6–7 presentations of a target detection stimulus were presented in each run. The target detection stimulus was an image of a house that appeared in the center of the screen, and not during a trial. Participants were instructed to press a button when they saw the house image. For data to be included in final analyses, participants were required to detect the target on at least 80 % of trials (all participants met these criteria).

2.4. Measures

2.4.1. Screen for Child Anxiety Related Emotional Disorders (SCARED)

Parent and child reports of anxiety symptoms were collected using the SCARED (Birmaher et al., 1997; see Table 1 for details). Items are rated on a 3-point Likert scale ranging from 0 (not true or hardly ever true) to 2 (true or often true). The SCARED produces a total score (41 items) and five symptom dimensions (generalized anxiety, social anxiety, panic, separation anxiety, and school anxiety). The SCARED has been shown to be a reliable and valid measure of child and adolescent anxiety symptomatology (Birmaher et al., 1999; Monga et al., 2000), and higher scores have been associated with greater symptom severity and functional impairment (DeSousa et al., 2013). Parent and child versions are identical in content.

2.4.2. Magnetic imaging acquisition

Neuroimaging was completed on a 3 T GE Scanner using a 32-channel head coil. Each functional imaging run consisted of 193 whole-brain (forty 4-mm axial slices) T*2-weighted echoplanar images (TR = 2000 milliseconds, TE = 25, flip angle = 60°, 24 field of view = 100). A

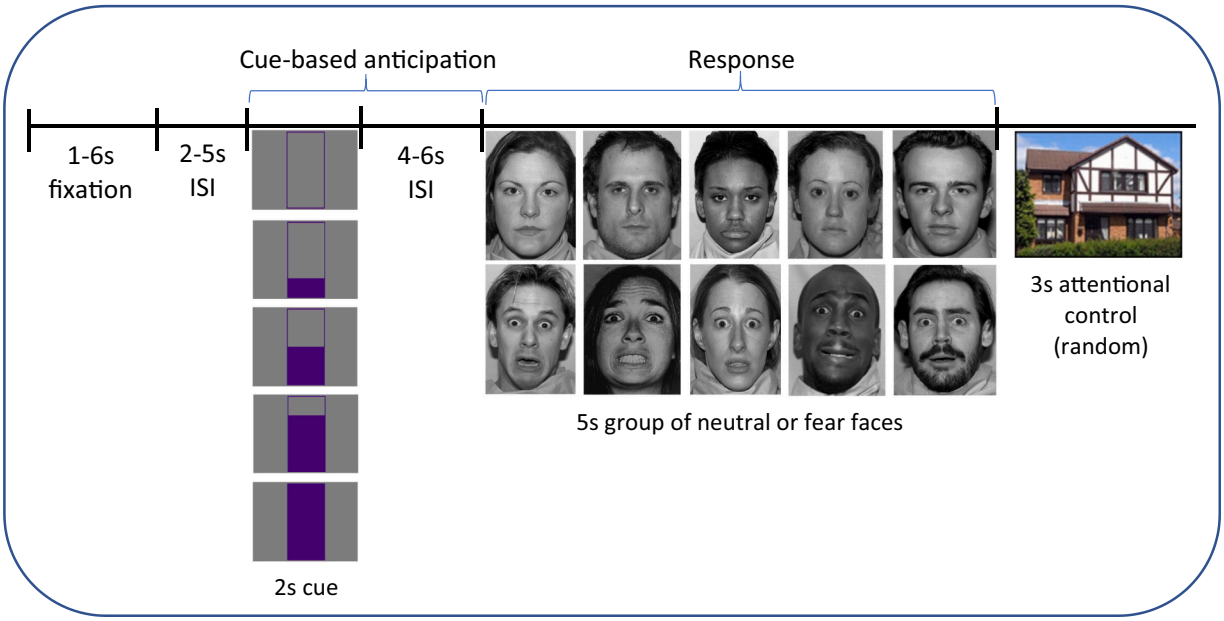

Fig. 1. Threat anticipation task.
Trial structure. Each trial consisted of a visual predictive cue (0 %, 25 %, 50 %, 75 %, and 100 % level color bars) followed by a 4–6 s anticipatory delay and 5 s of either 5 neutral or 5 fear faces presented sequentially. At random intervals, participants pressed a button to indicate the presence of a house. (For interpretation of the references to color in this figure legend, the reader is referred to the web version of this article.)

structural magnetization-prepared rapid acquisition gradient echo (MPRAGE) sequence was acquired for coregistration. A structural scan was collected in the sagittal direction (TI/TE = 425/min full, 1-mm slices, flip angle = 7°, 256 × 256 matrix).

2.4.3. Imaging analyses

All imaging analyses were conducted using AFNI_22.0.02 (Cox, 1996). Preprocessing (afni.proc.py) included despiking, slice time correction, coregistration, spatial smoothing with a 6-mm full-width half maximum smoothing kernel, and warping to standard MNI space. Resultant parameter estimates were converted to percentage signal change. The normalized percent signal change maps were spatially smoothed using a 6-mm FWHM Gaussian kernel. TRs with >1 mm of movement were censored. All included participants had >80 % of TRs in each run following censoring. At the individual subject level, single-subject time series were analyzed using a general linear model with separate regressors for the cued anticipation and face periods, formed by convolving stimulus functions (2-s cue, 5-s face) with a canonical hemodynamic response function. A total of twelve regressors were included in the subject-level modeling (AFNI, 3dDeconvolve). Six regressors, as described below, representing the three cue conceptual regressors (threat uncertainty, threat/safety certainty, threat probability), and face regressors for the fear and neutral faces, and a regressor for the target detection house. The six canonical motion regressors were also included in the subject-level model. We performed voxel-wise *t*-tests (AFNI 3dttest++) across all subjects and between groups to examine hypothesized differences in percent signal change during the cue and face periods, including age, sex, and mean-centered motion as covariates.

Whole-brain analyses for all contrasts were corrected with a voxel-wise threshold of $p < .005$, within a sample-specific gray matter (GM) mask. To create the GM mask, the MNI152_2009c anatomical template was segmented into GM and non-GM. Masked output maps included gray matter voxels of the whole brain. Significance for all output maps was determined in AFNI's 3dClustsim program using the ACF option (http://afni.nimh.nih.gov/pub/dist/doc/program_help/3dClustSim.html). Based on 10,000 Monte Carlo simulations, the minimum cluster size of 124 voxels was estimated by using the GM mask, the sample-mean ACF values, and a voxel-wise threshold of $p < .005$ to yield a whole-brain-corrected value of $p < .05$.

In addition to whole-brain analyses, as prior work using similar parameters linked uncertain anticipation to the amygdala and anterior insula (Krain et al., 2008; Morriss et al., 2019a, 2019b; Williams et al., 2015), further analyses were restricted to voxels within the amygdala and anterior insula. We accounted for multiple comparisons using a small volume correction within these targeted regions of interest (ROIs). Correction for multiple comparisons was identical to the whole-brain analyses conducted in the 3dClustSim program within AFNI. Results of the 3dClustSim indicated a voxel-wise threshold of $p < .005$ to yield a whole-brain-corrected value of $p < 0.05$combined with a minimum cluster size of 8 voxels for the bilateral amygdala and a minimum cluster size of 12 voxels for bilateral anterior insula.

2.5. Data analysis plan

2.5.1. Analysis 1a. Uncertainty processing during threat anticipation across all youth

Given our focus on uncertain threat anticipation, the first study goal was to identify regions involved in uncertainty processing across the entire youth sample using trial-level amplitude modulation. This creates two parameter estimates, one for the constant term (mean response) and one for amplitude modulation (difference from the mean). A whole-brain subject-level regression analysis (AFNI's 3dDeconvolve, using AM2) modeled threat uncertainty using a constant term across cues 25 %, 50 %, and 75 % (i.e., Threat Uncertainty Condition), and a second term included a regressor in which degree of uncertainty is weighted, with 25 % and 75 % weighted as 1 and 50 % weighted as 2 (i.e., Threat Uncertainty Modulated Condition). Including the amplitude modulation term enabled us to examine trial-by-trial associations between variation in blood oxygenation level-dependent (BOLD) response and variation in the *degree* of uncertainty in the cues. Regression coefficients for the amplitude modulation effects index the strength of the uncertainty-BOLD association. This was followed by a group analysis using a one group *t*-test, including age, sex, and mean-centered motion as covariates to examine effects across the whole sample.

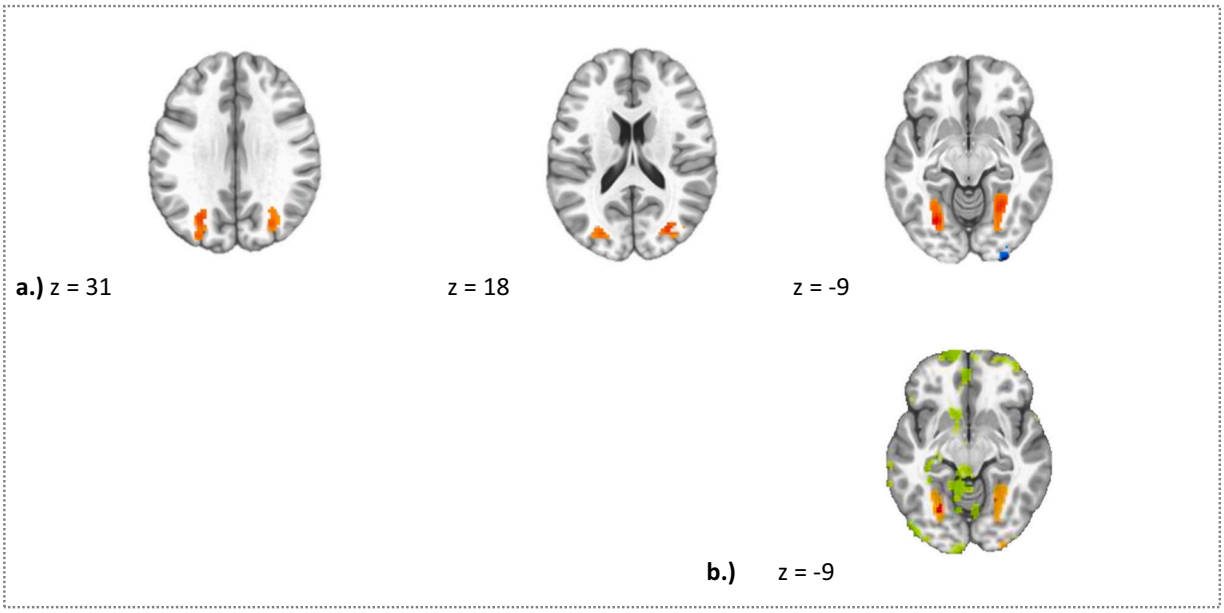

Fig. 2. Neural response to threat uncertainty: all youth.
a.) Results of a whole-brain analysis ($p < .005$, k > 124 voxels derived from a gray matter mask) show significant effects in bilateral inferior parietal cortex (R: 30, −77, 18; k = 902 voxels; L: 28, −72, 31; k = 716 voxels), bilateral fusiform gyrus (R: 28, −57, −10, k = 188 voxels; L: −28, −69, −10; k = 149 voxels), and middle occipital gyrus (35, −89, 2; k = 161 voxels) across all threat uncertainty cues (25 %, 50 %, 75 %). b.) Stability of fusiform gyrus for the threat uncertainty contrast in healthy adults. Image shows several stable regions of activation (in green, not cluster-thresholded for visualization purposes). Overlap between the stable activation in healthy adults and group-based youth results are shown in red. Group based results are added in yellow. (For interpretation of the references to color in this figure legend, the reader is referred to the web version of this article.)

2.5.2. Analysis 1b. Threat/safety certainty processing during threat anticipation across all youth

To further isolate neural response to uncertainty, we identified regions sensitive to threat/safety certainty across the entire youth sample. A whole-brain subject-level regression analysis modeled threat/safety certainty using a constant term across cues 0 % and 100 % (i.e., Threat/Safety Certainty Condition), followed by a group analysis using a one group *t*-test, including age, sex, and mean-centered motion as covariates to examine effects across the whole sample.

2.5.3. Analysis 2. Threat probability processing during threat anticipation across all youth

To examine neural processing associated with threat probability, we used the same approach as in the uncertainty analysis. Whole-brain subject-level models modeled a constant term across cues 25 %, 50 %, 75 %, and 100 % (i.e., Threat Probability Condition). A second term (the "modulated" term) included a regressor in which degree of upcoming threat is weighted linearly, with 25 % weighted as 1, 50 % weighted as 2, 75 % weighted as 3, and 100 % weighted as 4 (i.e., Threat Probability Modulated Condition). Including a linear amplitude modulation by trial-wise probability of the likelihood of fear faces allowed us to examine trial-by-trial associations between variation in BOLD response and variation in the degree of threat probability. Regression coefficients for the amplitude modulation index the strength of the cued threat probability-BOLD association. This was followed by a group analysis using a one group *t*-test, including age, sex, and mean-centered motion as covariates to examine effects across the whole sample.

2.5.4. Analysis 3. Anxious vs healthy comparisons

Third, and most critically, our final goal was to test the hypothesis that AD would be associated with magnitude of anticipatory responses to uncertainty and threat probability. To examine the impact of AD on threat uncertainty and threat probability processing during threat anticipation, participants were categorized into two groups based on the presence or absence of an AD. Youth with an AD diagnosis had higher current anxiety symptoms (SCARED Total scores, averaged across child and parent reports) than healthy youth ($t(50) = 9.084, p < .001$). Groups did not differ in sex ($\chi^2(1) = 1.87$, $p = .172$), or IQ (Wechsler, 1999) ($t(48) = 1.05$, $p = .297$), but AD youth were younger in age ($t(50) = -2.805$, $p = .007$); as noted, age was used as a nuisance covariate in all analyses.

For the neuroimaging results, we used 3dttest++ with the same covariates as the one-group *t*-tests to contrast the differences in the anxious compared to healthy participants across all conditions (i.e., Threat Uncertainty, Threat Uncertainty Modulated, Threat/Safety Certainty, Threat Probability, Threat Probability Modulated).

As prior work suggests differential recruitment of amygdala and vmPFC during uncertain threat cross age (Ganella et al., 2018; Morriss et al., 2019a, 2019b), we conducted exploratory analyses to probe any effects of age on our contrasts of interest (uncertainty processing, threat/safety processing, threat probability processing) by collapsing across the two groups (healthy, AD) and examining the effects of age as continuous variable, while controlling for group.

Supplementary analyses also identified regions reactive to the aversive stimuli (fear faces relative to baseline and relative to neutral faces) and during target detection (house) for the entire group and for AD vs healthy youth. As these contrasts were not the primary focus of this study, results are presented in Supplementary Materials.

2.6. Reliability analysis

To complement our fMRI study in AD vs healthy youth, a companion reliability study considered fMRI data collected in an independent sample of 19 healthy adults aged 20 to 45 years (M = 27.01, SD = 7.23 at the first scan). All adult participants completed the anticipation task three times on separate occasions across three geographic locations (NIMH, University of Wisconsin, Madison, and Vanderbilt University Medical Center). Site order was randomized across participants using a random number generator. With this approach, one third of the sample underwent the first scanning session at each of the three study sites.

Table 2
Uncertainty condition (constant term of ambiguity across cues 25, 50, 75).

Region	Cluster size	MNI coordinates			*t* value	Mean ICC[a]
	Voxels	x	y	z		
All youth						
Precuneus	902	30	−77	18	5.30	–
	716	−28	−72	31	5.22	–
Fusiform gyrus		28	−57	−10	5.58	0.37
		−28	−69	−10	6.44	0.34
Middle occipital gyrus	161	35	−89	−2	5.72	0.36
Anxious vs healthy comparison						
vlPFC/BA 47	140	43	46	−15	4.46	0.42

Note: whole brain cluster threshold: $p = .005$, $k > 124$ voxels. ICC = intraclass correlation coefficient.
[a] Average ICC values calculated in $n = 19$ healthy adults across the overlapping cluster (ICC > 0.29).

Bayesian linear mixed-effects models (3dLME; Chen et al., 2018; Haller et al., 2022) were used to compute a voxel-wise intra-class correlation coefficient (ICC) of BOLD activation across the three sites. The Bayesian ICC approach has been shown to overcome potential issues in traditional ICC estimates (e.g., negative ICC values, missing data, confounding effects) (Haller et al., 2022). Analyses were performed on all significant contrasts that emerged from youth group analyses in AFNI using subject and site as random variables in the model. For all contrasts, ICCs were modeled with a 2-way mixed model with absolute agreement [i.e., ICC (2,1)]. The initial ICC threshold value was set to 0.29, falling within 95 % CI measures calculated from 19 subjects and three repeated measures (i.e., visits). We elected to use the same cluster correction used in our youth group study. Average ICC values within each cluster that was significant in the youth sample appear in tables for each contrast. Individual level contrasts from the BOLD GLMs were used as input in the ICC analyses. A whole-brain GM mask was used for the ICC analysis to parallel group analyses. Figures present voxels that contain significant ICC values in the adult group, significant group effects in youth, and their overlap.

3. Results

3.1. Analysis 1a. Neural response to threat uncertainty during threat anticipation across all youth

To isolate neural response to threat uncertainty during threat anticipation, whole-brain analyses examined: (1) an overall response to cues signaling threat uncertainty during the threat anticipation period (i.e., a constant term across cues signaling 25 %, 50 %, and 75 % probability of viewing negative emotional faces) and (2) a modulated response to cues signaling threat uncertainty during the threat anticipation period (i.e., a modulated term with maximum weight at the 50 % cue, and intermediate weights at the 25 % and 75 % cues). We observed robust response across all threat uncertainty cues (i.e., one term across 25 %, 50 %, 75 %) in bilateral precuneus, bilateral fusiform gyrus, and

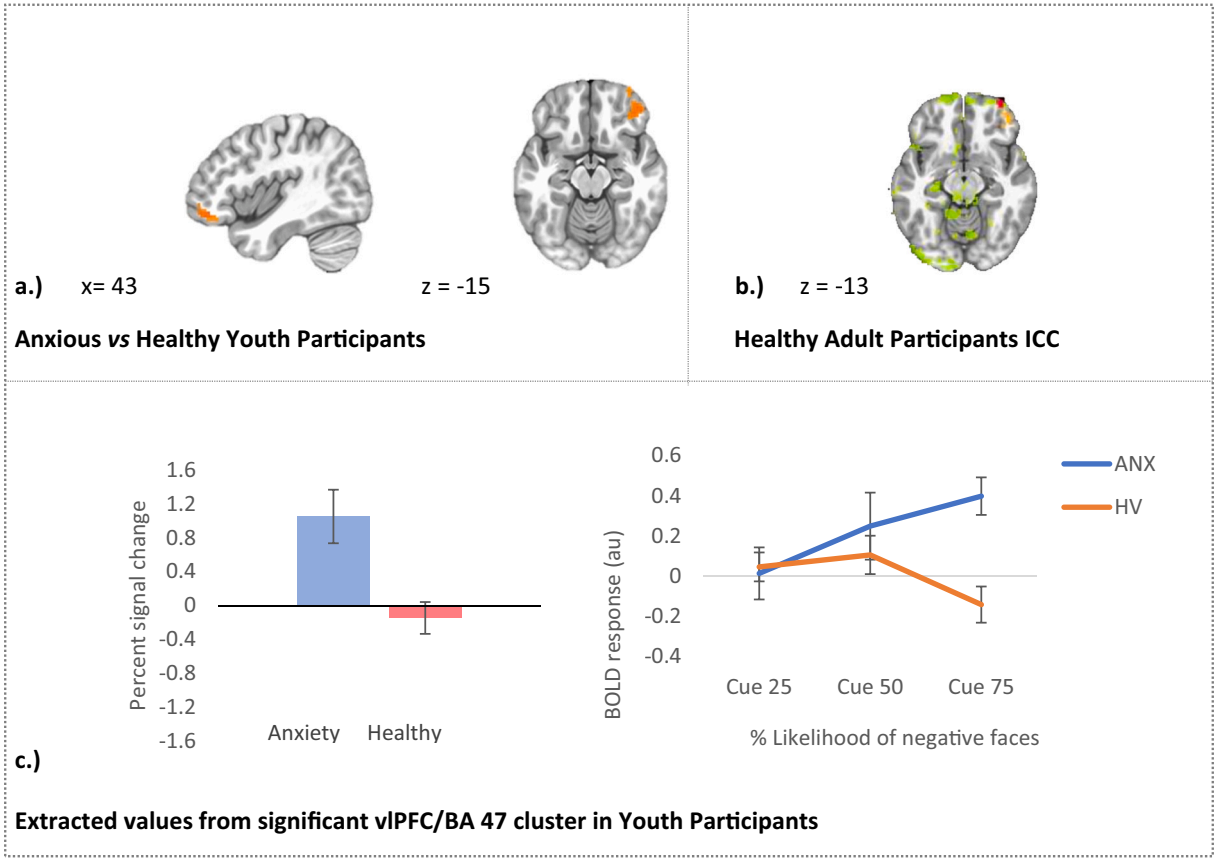

Fig. 3. Neural response to threat uncertainty: anxious vs healthy children.
a.) Results of a whole-brain analysis ($p < .005$, k > 124 voxels derived from a gray matter mask) reveal a significant effect in ventrolateral PFC/BA 47 (43, 46, −15) for anxious relative to healthy child participants across all threat uncertainty cues (25 %, 50 %, 75 %). b.) Stability of event-related middle vlPFC/BA 47 activation in healthy adults. Image shows several stable regions of activation (in green, not cluster-thresholded for visualization purposes). Overlap between the stable activation in healthy adults and group-based youth results are shown in red. Group based child results are added in yellow. c.) Plots of BOLD signal change from the associated PFC/BA 47 activation cluster in youth. (For interpretation of the references to color in this figure legend, the reader is referred to the web version of this article.)

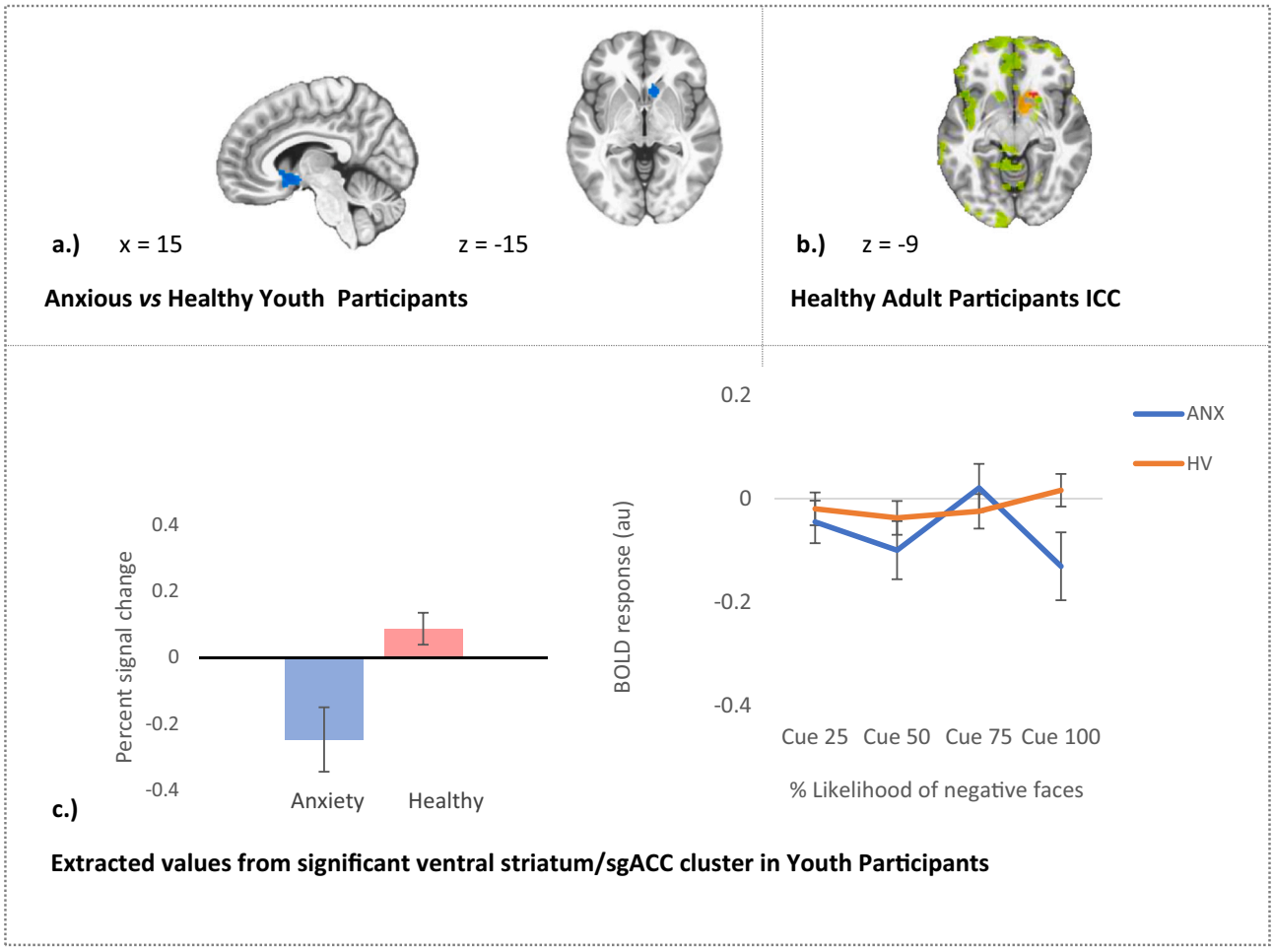

Fig. 4. Neural response to threat probability: anxious vs healthy.
a.) Results of a whole-brain analysis ($p < .005$, >124 voxels derived from a gray matter mask) reveal a significant effect in right ventral striatum (in blue) (15, 19, −3) extending into subgenual ACC for anxious relative to healthy participants. b.) Stability of ventral striatum/sgACC activation in healthy adults. Image shows several stable regions of activation (in green, not cluster-thresholded for visualization purposes). Overlap between the stable activation in healthy adults and group-based youth results are shown in red. Group based results are added in yellow. c.) Plots of BOLD signal change from the associated PFC/BA 47 activation cluster in youth. (For interpretation of the references to color in this figure legend, the reader is referred to the web version of this article.)

lingual gyrus, as well as reduced activation within regions of the middle occipital gyrus (Fig. 2, Table 2; $p < .005$, corrected). No significant effect emerged for the modulated threat uncertainty term for the full youth sample.

3.2. Analysis 1b. Neural response to certain cues during anticipation across groups

To isolate the neural response to threat/safety certainty during threat anticipation, whole-brain analyses examined the overall response to cues signaling threat/safety certainty during the threat anticipation period (i.e., a constant term across cues signaling 0 % and 100 % probability of viewing negative emotional faces). We observed robust response in right superior parietal lobule/precuneus, bilateral fusiform gyrus, right middle frontal gyrus, and lingual gyrus, as well as reduced activation within regions of the middle occipital gyrus (Table 2).

3.3. Analysis 2. Neural response to threat probability during threat anticipation across groups

To isolate the effects of threat probability on neural response during threat anticipation, whole-brain analyses examined: (1) an overall response to cues signaling threat probability during the threat anticipation period (i.e., a constant term across cues signaling 25 %, 50 %, 75 %, and 100 % probability of viewing negative emotional faces) and (2) a modulated response to cues signaling threat probability during the threat anticipation period (i.e., a modulated linear term with minimum weight at the 25 % cue, and maximum weight at the 100 % cue). No significant effects for the average term across threat cues, or the linearly modulated term across threat cues during the cued threat anticipation period emerged for the full youth sample.

3.4. Analysis 3. Anxious vs healthy

We first tested the hypothesis that youth with ADs have altered neural activation in amygdala, anterior insula, and OFC during anticipation of uncertain threat, both as at the average threat level and as a function of threat level. To do so, we compared AD youth and healthy controls for their difference in activation to the uncertainty (constant term) and modulated uncertainty (modulated term) regressors. Contrary to our predictions, we observed no group differences in amygdala or anterior insula activation in either of these conditions.

However, three other notable findings emerged for these contrasts. First, youth with ADs had greater activation to uncertainty in ventrolateral PFC (vlPFC)/Brodmann's Area 47 (Fig. 3, Table 2). Decomposition of this difference shows greater BOLD response in AD youth from to 25 % to 75 % threat likelihood (Fig. 3, panel D). Second, youth with ADs relative to healthy controls demonstrated deactivations to threat cues

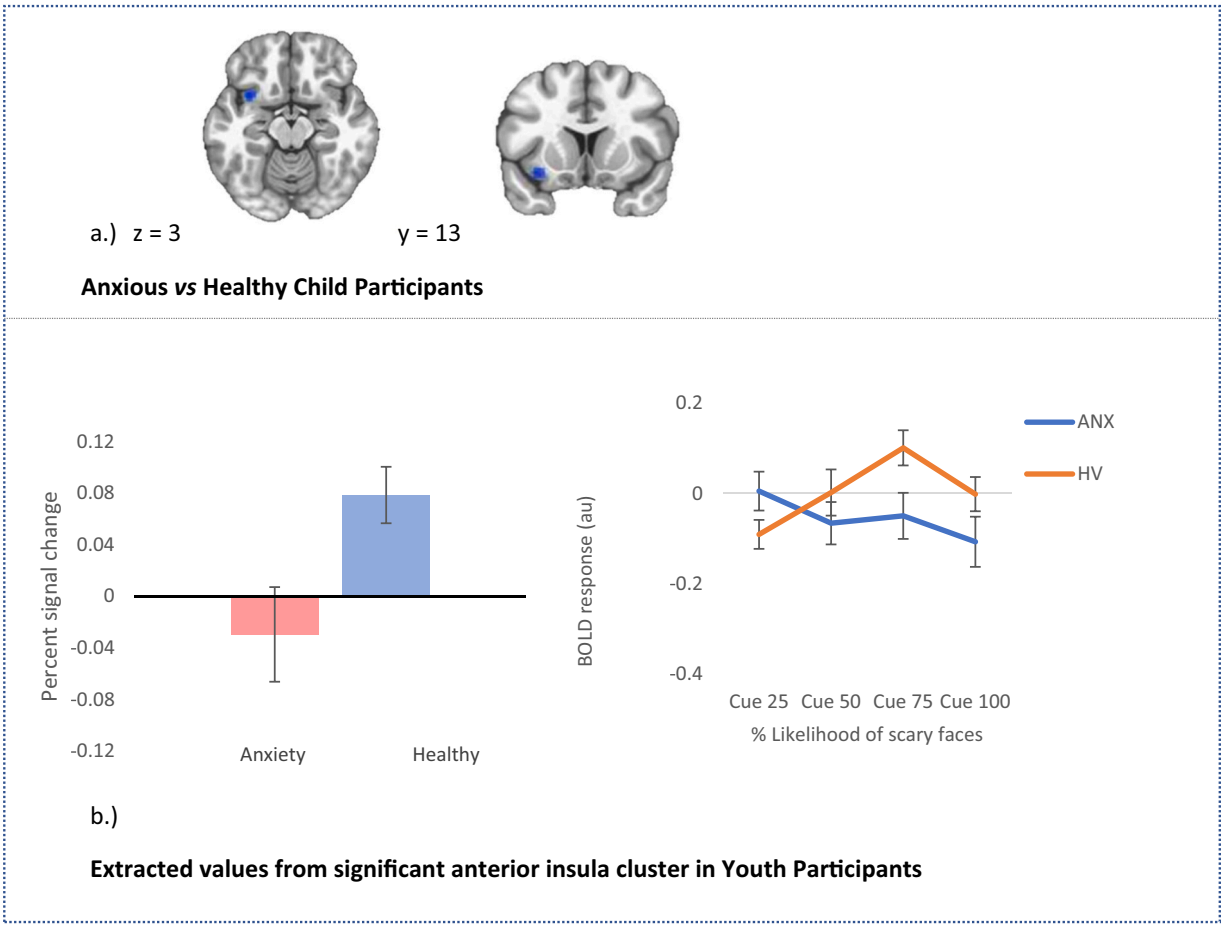

Fig. 5. Neural response to modulated threat probability: anxious vs healthy.
a.) Results of a whole-brain analysis ($p < .005$, k < 12 voxels small volume corrected) reveal a significant effect in left anterior insula (−33, 13, 15) for anxious relative to healthy participants. b.) Plots of BOLD signal change from the associated PFC/BA 47 activation cluster in youth.

(constant term across 25 %, 50 %, 75 %, and 100 % cues) in ventral striatum/subgenual ACC (sgACC) (Fig. 4, Table 4). This effect appears to be driven primarily by the highest likelihood of experiencing the aversive stimuli. Third, as shown in Fig. 5, within the Modulated Threat Probability condition (i.e., linear modulation of threat probability), AD youth demonstrated significant deactivations in anterior insula (−33, 13, 15, $p < .05$ svc, bilateral anterior insula mask) that were absent in the healthy group. No group differences emerged in amygdala or anterior insula using svc.

Exploratory analyses probing continuous age effects across the entire sample on our contrasts of interest (uncertainty processing, threat/safety processing, threat probability processing), while controlling for group, yielded no significant clusters following cluster correction.

3.5. ICC analysis

There were areas of overlap of the ICC values in the adults and group effects in youth in the Threat Uncertainty and Threat Probability conditions. However, of note, reliability was modest [0.29 threshold]. No such overlap arose for the Threat Probability Modulated condition. Specifically, significant ICCs were observed in bilateral fusiform gyrus for all subjects in the Threat Uncertainty condition, in right vlPFC/BA 47 for AD vs healthy youth in the Threat Uncertainty condition, and right ventral striatum/sgACC for AD vs healthy youth in the Threat Probability condition. These overlaps are presented in Figs. 2b, 3b, and 4b. Additional information on ICC analyses is presented in Supplemental Materials.

4. Discussion

Excessive fear responses in the face of uncertain threat are central in clinical anxiety. Although previous work has compared behavioral and neural responding between certain versus uncertain cued threat outcomes (Hiser et al., 2021; Hur et al., 2020; Krain et al., 2006; Krain et al., 2008; Radoman et al., 2021; Somerville et al., 2013), few studies have examined responses to varying levels of threat uncertainty, particularly among youth. The current fMRI study first examined whether youths' anticipatory neural responses scale with levels of threat probability. Findings should be considered preliminary, based on the small sample size, appropriate for a first report of a novel task. The study next considered whether youth with and without AD differ both in their overall response to uncertain threat and in their response to varying levels of potential threat. Finally, to evaluate psychometric properties of this new task, the study examined cross-site test-retest reliability of task effects in an independent group of healthy adults.

Results suggest the potential utility of studying uncertain threat anticipation in anxious youth to inform treatment development. Specifically, uncertain threat anticipation engaged bilateral inferior parietal cortex, fusiform gyrus, and lingual gyrus across all youth, whereas relative to healthy youth, AD youth exhibited greater activation in vlPFC/BA47. Further, AD differed from healthy youth in scaling of ventral striatum/sgACC activation with threat probability. Finally, AD relative to healthy youth displayed divergent patterns of scaling in anterior insula with escalating threat probability. Complementing these results, significant, albeit modest, cross-site test-retest reliability in these regions was observed in an independent sample of healthy adults.

Findings in fusiform gyrus and parietal cortex during threat anticipation across the sample are consistent with predictive coding models, such as the Embodied Predictive Interoception Coding model (EPIC, Barrett & Simmons, 2015). According to this model, so-called *interoceptive predictions*—autonomic modulatory commands— enable predictions of incoming sensory inputs. Interoceptive predictions are matched with actual sensory information, and this information is modulated to match the predicted states. This perspective could explain the observed engagement of the fusiform gyrus, a face-processing area, in the absence of any face stimuli during the threat anticipation period. Thus, threat cues may drive youth's interoceptive predictions during uncertain threat anticipation and plausibly induce changes in visual processing areas in anticipation of incoming visual facial information (Hiser et al., 2021; see also Glenn et al., 2020, for interactions between affective and visual neurocircuitry).

Contrary to expectations, AD youth did not differentially engage the amygdala or anterior insula when viewing cues signaling threat uncertainty. While this differs from previous research (Morriss et al., 2015; Schienle et al., 2010; Shankman et al., 2014; Simmons et al., 2008; Somerville et al., 2013; Williams et al., 2015), small sample size could account for such unexpected findings. Moreover, features of our design also may contribute to these unexpected results. In the current study, an image of a house was presented as a detection target to promote attention. This may have overly focused AD youth on "getting the task right", distracting from non-target aspects of the task. Further, we examined the uncertainty parameter of risk, which is generally considered to be less aversive than the parameter of ambiguity (Chen and Lovibond, 2016; Morriss et al., 2022a), and may account for discrepant findings. Likewise, more robust aversive stimuli may elicit stronger anxiety differences in anticipatory responding (Abend et al., 2021b, though see Michalska et al., 2018). Finally, whereas the current study relied only on outcome uncertainty under the parameter of risk (Kobayashi and Hsu, 2017; Payzan-LeNestour and Bossaerts, 2011) about a particular threat, several prior studies included multiple sources of uncertainty, such as whether, when, and what type of threat would be presented (Schienle et al., 2010; Shankman et al., 2014; Simmons et al., 2008). Such multiple parameters of uncertainty presented at the same time (e.g., outcome and temporal uncertainty) may be more evocative for anxious individuals (Morriss et al., 2020; Morriss et al., 2021a, 2021b; Morriss et al., 2022b). Indeed, a recent study using only outcome as a source of uncertainty observed no differential engagement of the amygdala or anterior insula as a function of intolerance of uncertainty (IU), a common feature of anxiety, and instead documented greater recruitment of dorsal and medial prefrontal cortex to uncertain threat cues in individuals with higher IU (Morriss et al., 2021a, 2021b). However, previous studies (Feola et al., 2021; Krain et al., 2008; Williams et al., 2015) including only a single source of uncertainty did observe heightened amygdala engagement, particularly among AD youth high on intolerance of uncertainty (Krain et al., 2008). As with the present study, two of these studies (Krain et al., 2008; Williams et al., 2015) employed instructed uncertainty in their designs and thereby assessing the risk parameter, whereas Feola et al. (2021) assessed the ambiguity parameter. Thus, other differences between the current study and prior work may account for the discrepant findings.

The current study adapted procedures from Williams et al. (2015), which examined responding to uncertain versus certain threat in a dichotomous manner. In that study, the difference between the uncertain and certain conditions was large (e.g., a 50 % difference in probability), in contrast to the parametric variation in the current study. By design, the current study employed a broader range of threat probability, to mirror uncertain conditions youth may encounter in daily life. Thus, both salience and informational value contained within any specific probability may be diluted compared to a dichotomous cue. Our results need to be further extended to fully understand how anxiety modulates neural circuitry under different task demands and parameters of uncertainty.

AD was associated with greater recruitment of the vlPFC/BA47 to uncertain threat cues. As BA47 is generally involved in response inhibition and cognitive control (Casey et al., 2001; FeldmanHall et al., 2019; O'Doherty et al., 2003; Schoenbaum & Roesch, 2005) and specifically involved in regulation of fear (Shiba et al., 2016), anxious youth may have been more cautious or regulated when experiencing uncertainty about upcoming threat. The current study collected no data concerning youths' autonomic responses (Michalska et al., 2019) or degrees of explicit emotion regulation during scanning. Experimentally manipulating task instructions to prompt regulatory strategies during threat anticipation would help refine our understanding of the processes underlying these findings. Research in decision making may provide additional clues. This work has argued that BA47 is involved in key aspects of decision-making, such as assigning "risk" value to a stimulus under uncertain conditions (Rangel et al., 2008; Windmann et al., 2006). Even though the current study did not require participants to make decisions following threat cues, enhanced engagement of this regulatory structure in AD youth suggests that hyperactivity in vlPFC/BA47 could act as a compensatory mechanism under conditions of uncertainty.

Relative to healthy youth, youth with AD exhibited deactivation in ventral striatum/sgACC to all cues signaling threat probability (i.e., a constant term across 25 %, 50 %, 75 %, and 100 % cues). Recent meta-analytic evidence suggests that ventral striatum and ACC are commonly involved in the anticipation of aversive stimuli across sensory modalities (Andrzejewski et al., 2019). Other work has implicated the ventral striatum in initiating motor responses to affectively salient stimuli (Greenberg et al., 2015; Rolls, 2000). Thus, ventral striatum and ACC are part of a larger neural network for initiating preparatory responding in anticipation of threat.

Whereas group differences emerged in neural response to *overall* levels of uncertainty, we did not observe neural response *modulation* when considering escalating levels of threat uncertainty (i.e., maximal at 50 %) — either at the group level or between AD and healthy youth. In contrast, one prior EEG study, which used a threat of shock paradigm, reported that participants higher in intolerance to uncertainty, exhibited greater differences in the P200, an early attentional waveform, across levels of uncertainty in adults (Tanovic et al., 2018). This apparent discrepancy may be due to the salience of the stimuli (electric shocks) that were used in their study, which may have captured attention soon after cue onset. Even though they are survival-relevant, the pictorial stimuli in our study may have been less motivationally salient than threat of shock, thus exhibiting less fine-grained fluctuations in response to threat probability. Since the majority of prior studies do not modulate levels of threat probability at this level of specificity, future neuroimaging research might build on these findings and examining the role stimulus salience plays in modulating threat responses.

Examining responding to varying levels of threat uncertainty may be relevant for understanding risk for anxiety. In the present study, while we did not observe group differences in amplitude modulation for cues signaling threat uncertainty, we did observe attenuated modulation in anterior insula for cues signaling threat probability among AD relative to healthy youth (Fig. 5). Given the known role of the anterior insula in interoceptive processing (Craig and Craig, 2009), our data could suggest that AD youth are less attuned to bodily sensations or less able to flexibly modulate interoceptive signals in anticipation of threat (e.g., Paulus & Stein, 2010).

To complement our study in youth, we also examined test-retest reliability of brain regions engaged by our task in a separate sample of healthy adults tested at three different sites. Significant, albeit low, stability in regions showing the highest mean level of activation in the youth sample was established across three of the four significant contrasts. On threat uncertainty trials (i.e., constant term across 25 %, 50 %, and 75 % cues) that showed increased activation in all youth subjects, activation in fusiform gyrus showed significant reliability in adults. On threat uncertainty trials where between-group differences emerged in youth, vlPFC/BA47 likewise showed significant reliability. Given that

Table 3
Certainty condition (constant term of certainty across cues 0, 100).

Region	Cluster size	MNI coordinates			*t* value	Mean ICC[a]
	Voxels	x	y	z		
All youth						
Superior parietal lobule	2830	28	−57	46	7.44	0.56
Middle occipital gyrus	425	28	−89	−5	−9.22	0.46
	342	−18	−97	−7	−8.69	0.38
Fusiform gyrus	357	28	−52	−12	8.43	0.35
	204	−30	−62	−10	6.52	0.37
Middle frontal gyrus	226	38	8	43	4.73	0.37
Lingual gyrus	127	0	−79	1	4.70	–

Note: whole brain cluster threshold: $p = .005$, $k > 124$ voxels. ICC = intraclass correlation coefficient.
[a] Average ICC values calculated in n = 19 healthy adults across the overlapping cluster (ICC > 0.29).

Table 4
Threat condition (constant term of threat across cues 25, 50, 75, 100).

Region	Cluster size	MNI coordinates			*t* value	Mean ICC[a]
	Voxels	x	y	z		
Anxious vs healthy comparison						
Ventral striatum/ subgenual ACC	161	15	18	−15	−5.34	0.37

Note: whole brain cluster threshold: $p = .005$, $k > 124$ voxels. ICC = intraclass correlation coefficient.
[a] Average ICC values calculated in $n = 19$ healthy adults across the overlapping cluster (ICC > 0.29).

prior uncertainty research has documented differences in vlPFC activation between anxious and nonanxious individuals (e.g., Monk et al., 2006), perturbed vlPFC/BA47 engagement may represent a promising biomarker. Further, on threat probability trials (i.e., constant term across 25 %, 50 %, 75 %, and 100 % cues) where group differences emerged in ventral striatum, significant reliability was observed in the adult sample. We note that our reliability values, while significant, were rather low (range 0.22–0.55, see Tables 2 and 3). Thus, establishing adequate reliability is important and may justify further youth-focused research on vlPFC engagement across different threat anticipation tasks.

5. Limitations

Several limitations of the current study should be acknowledged. First, this was a cross-sectional study; a longitudinal design would allow stronger inferences about causal processes. Second, because our AD group was small, we may have been insufficiently powered to detect subtle effects. Since our study was based on sample considerations in the Williams et al. (2015) study and we did not formally conduct an a-priori power analysis when we designed our study, it would be analytically misleading to retrospectively calculate power for outcomes already observed (Chen et al., 2022; Zhang et al., 2019). We believe that the test-retest approach in our companion sample of adults mitigates some concern in that we probe a-priori regions of interest that differentiate between healthy vs anxious youth and also show test-retest reliability in adults. Nevertheless, replication using this modified task is important in larger samples and is currently underway. Third, threat anticipation was examined only across neural levels of responding. Key features in anxiety are subjective/cognitive experiences and physiological responding (Abend et al., 2021a; Michalska et al., 2022; Taschereau-Dumouchel et al., 2022); future work should assess subjective uncertainty during threat anticipation as well as physiological threat responding. Fourth, we did not collect a youth IU measure (see e.g., Krain et al., 2006, 2008; Osmanağaoğlu et al., 2018). IU, distress resulting from the possibility that adverse events may occur unpredictably, has been identified as an important cognitive vulnerability for the development and maintenance of maladaptive anxiety (Boelen and Reijntjes, 2009; Boswell et al., 2013; Carleton et al., 2012; Carleton, 2016) and may have provided additional traction into the nature of anxiety-linked neural responses to uncertainty. Finally, this study included only behavioral responses to a target detection component; extension with different behavioral tasks probing responses to uncertainty (e.g., behavioral avoidance or information seeking under uncertain conditions) is an important next step.

6. Conclusions

Greater engagement of vlPFC/BA47 during uncertain threat anticipation in general is associated with anxiety disorders in middle childhood and adolescence. This engagement is accompanied by reduced ventral striatum activation during threat probability and attenuated flexibility of responding during parametric uncertain threat in anterior insula in anxious youth. Moreover, we relate group level findings to task reliability in adults. The findings extend understanding of uncertain anticipation in anxiety.

Data availability

Data will be made available on request.

Acknowledgements

Supported by National Institute of Mental Health Intramural Research Program Project number ZIAMH00278.

Appendix A. Supplementary data

Supplementary data to this article can be found online at https://doi.org/10.1016/j.ijpsycho.2022.07.006.

References

Abend, R., Bajaj, M.A., Coppersmith, D.D., Kircanski, K., Haller, S.P., Cardinale, E.M., Pine, D.S., 2021a. A computational network perspective on pediatric anxiety symptoms. Psychol. Med. 51 (10), 1752–1762.
Abend, R., Bajaj, M.A., Harrewijn, A., Matsumoto, C., Michalska, K.J., Necka, E., Pine, D. S., 2021b. Threat-anticipatory psychophysiological response is enhanced in youth with anxiety disorders and correlates with prefrontal cortex neuroanatomy. J. Psychiatry Neurosci. 46 (2), E212–E221.
Adolphs, R., 2013. The biology of fear. Curr. Biol. 23 (2), R79–R93.
American Psychiatric Association, 2013. Diagnostic and Statistical Manual of Mental Disorders, 5th ed. American Psychiatric Association, Washington, DC.
Andrzejewski, J.A., Greenberg, T., Carlson, J.M., 2019. Neural correlates of aversive anticipation: an activation likelihood estimate meta-analysis across multiple sensory modalities. Cogn.Affect.Behav.Neurosci. 19 (6), 1379–1390.
Baker, A.E., Galván, A., 2020. Threat or thrill? The neural mechanisms underlying the development of anxiety and risk taking in adolescence. Dev.Cogn.Neurosci. 45, 100841.
Barlow, D.H., 2000. Unraveling the mysteries of anxiety and its disorders from the perspective of emotion theory. Am. Psychol. 55 (11), 1247.
Barlow, D.H., 2004. Anxiety and Its Disorders: The Nature and Treatment of Anxiety and Panic. Guilford Press.
Barrett, L.F., Simmons, W.K., 2015. Interoceptive predictions in the brain. Nat. Rev. Neurosci. 16 (7), 419–429.
Beesdo, K., Knappe, S., Pine, D.S., 2009. Anxiety and anxiety disorders in children and adolescents: developmental issues and implications for DSM-V. Psychiatr. Clin. 32 (3), 483–524.
Birmaher, B., Khetarpal, S., Brent, D., Cully, M., Balach, L., Kaufman, J., Neer, S.M., 1997. The screen for child anxiety related emotional disorders (SCARED): scale construction and psychometric characteristics. J. Am. Acad. Child Adolesc. Psychiatry 36 (4), 545–553.
Birmaher, B., Brent, D.A., Chiappetta, L., Bridge, J., Monga, S., Baugher, M., 1999. Psychometric properties of the screen for child anxiety related emotional disorders (SCARED): a replication study. J. Am. Acad. Child Adolesc. Psychiatry 38 (10), 1230–1236.
Boelen, P.A., Reijntjes, A., 2009. Intolerance of uncertainty and social anxiety. J. Anxiety Disord. 23 (1), 130–135.

Boswell, J.F., Thompson-Hollands, J., Farchione, T.J., Barlow, D.H., 2013. Intolerance of uncertainty: a common factor in the treatment of emotional disorders. J. Clin. Psychol. 69 (6), 630–645.
Carleton, R.N., Mulvogue, M.K., Thibodeau, M.A., McCabe, R.E., Antony, M.M., Asmundson, G.J., 2012. Increasingly certain about uncertainty: intolerance of uncertainty across anxiety and depression. J.Anxiety Disord. 26 (3), 468–479.
Carleton, R.N., 2016. Fear of the unknown: one fear to rule them all? J.Anxiety Disord. 41, 5–21.
Casey, B.J., Forman, S.D., Franzen, P., Berkowitz, A., Braver, T.S., Nystrom, L.E., et al., 2001. Sensitivity of prefrontal cortex to changes in target probability: a functional MRI study. Hum. Brain Mapp. 13, 26–33.
Chen, G., Taylor, P.A., Haller, S.P., Kircanski, K., Stoddard, J., Pine, D.S., Cox, R.W., 2018. Intraclass correlation: improved modeling approaches and applications for neuroimaging. Hum. Brain Mapp. 39 (3), 1187–1206.
Chen, G., Pine, D.S., Brotman, M.A., Smith, A.R., Cox, R.W., Taylor, P.A., Haller, S.P., 2022. Hyperbolic trade-off: the importance of balancing trial and subject sample sizes in neuroimaging. NeuroImage 247, 118786.
Chen, J.T.H., Lovibond, P.F., 2016. Intolerance of uncertainty is associated with increased threat appraisal and negative affect under ambiguity but not uncertainty. Behav. Ther. 47 (1), 42–53.
Chin, B., Nelson, B.D., Jackson, F., Hajcak, G., 2016. Intolerance of uncertainty and startle potentiation in relation to different threat reinforcement rates. Int. J. Psychophysiol. 99, 79–84.
Cox, R.W., 1996. AFNI: software for analysis and visualization of functional magnetic resonance neuroimages. Comput. Biomed. Res. 29 (3), 162–173.
Craig, A.D., Craig, A.D., 2009. How do you feel–now? The anterior insula and human awareness. Nat. Rev. Neurosci. 10 (1).
Davis, M., Walker, D.L., Miles, L., Grillon, C., 2010. Phasic vs sustained fear in rats and humans: role of the extended amygdala in fear vs anxiety. Neuropsychopharmacol. 35, 105–135.
DeSousa, D.A., Salum, G.A., Isolan, L.R., Manfro, G.G., 2013. Sensitivity and specificity of the Screen for Child Anxiety Related Emotional Disorders (SCARED): a community-based study. Child Psychiatry Hum. Dev. 44 (3), 391–399.
Ekman, P., Friesen, W., 2006. Pictures of Facial Affect. Consulting Psychologists Press, Palo Alto.
Elliott, M.L., Knodt, A.R., Ireland, D., Morris, M.L., Poulton, R., Ramrakha, S., Hariri, A. R., 2020. What is the test-retest reliability of common task-functional MRI measures? New empirical evidence and a meta-analysis. Psychol. Sci. 31 (7), 792–806.
FeldmanHall, O., Glimcher, P., Baker, A.L., , Nyu Prospec Collaboration, Phelps, E.A., 2019. The functional roles of the amygdala and prefrontal cortex in processing uncertainty. J. Cogn. Neurosci. 31 (11), 1742–1754.
Feola, B., Melancon, S.N.T., Clauss, J.A., Noall, M.P., Mgboh, A., Flook, E.A., Blackford, J.U., 2021. Bed nucleus of the stria terminalis and amygdala responses to unpredictable threat in children. Dev. Psychobiol. 63 (8), e22206.
Ganella, D.E., Drummond, K.D., Ganella, E.P., Whittle, S., Kim, J.H., 2018. Extinction of conditioned fear in adolescents and adults: a human fMRI study. Front. Hum. Neurosci. 647.
Glenn, D.E., Feldman, J.S., Ivie, E.J., Shechner, T., Leibenluft, E., Pine, D.S., Michalska, K.J., 2021. Social relevance modulates multivariate neural representations of threat generalization in children and adults. Dev. Psychobiol. 63 (7), e22185.
Glenn, D.E., Fox, N.A., Pine, D.S., Peters, M.A., Michalska, K.J., 2020. Divergence in cortical representations of threat generalization in affective versus perceptual circuitry in childhood: relations with anxiety. Neuropsychologia 142, 107416.
Gorka, S.M., Lieberman, L., Shankman, S.A., Phan, K.L., 2017. Startle potentiation to uncertain threat as a psychophysiological indicator of fear-based psychopathology: an examination across multiple internalizing disorders. J. Abnorm. Psychol. 126 (1), 8–18.
Greenberg, T., Carlson, J.M., Rubin, D., Cha, J., Mujica-Parodi, L., 2015. Anticipation of high arousal aversive and positive movie clips engages common and distinct neural substrates. Soc. Cogn. Affect. Neurosci. 10 (4), 605–611.
Grillon, C., 2008. Models and mechanisms of anxiety: evidence from startle studies. Psychopharmacology 199 (3), 421–437.
Grillon, C., Lissek, S., Rabin, S., McDowell, D., Dvir, S., Pine, D.S., 2008. Increased anxiety during anticipation of unpredictable but not predictable aversive stimuli as a psychophysiologic marker of panic disorder. Am. J. Psychiatr. 165 (7), 898–904.
Grupe, D.W., Nitschke, J.B., 2013. Uncertainty and anticipation in anxiety: an integrated neurobiological and psychological perspective. Nat. Rev. Neurosci. 14 (7), 488–501.
Haller, S.P., Chen, G., Kitt, E.R., Smith, A.R., Stoddard, J., Abend, R., Pagliaccio, D., 2022. Reliability of t ask-evoked neural activation during f ace-emotion paradigms: effects of scanner and psychological processes. Hum. Brain Mapp. 43 (7), 2109–2120.
Hiser, J., Schneider, B., Koenigs, M., 2021. Uncertainty potentiates neural and cardiac responses to visual stimuli in anxiety disorders. Biol.PsychiatryCogn.Neurosci. Neuroimaging 6 (7), 725–734.
Hur, J., Smith, J.F., DeYoung, K.A., Anderson, A.S., Kuang, J., Kim, H.C., Shackman, A.J., 2020. Anxiety and the neurobiology of temporally uncertain threat anticipation. J. Neurosci. 40 (41), 7949–7964.
Kaufman, J., Birmaher, B., Brent, D., Rao, U.M.A., Flynn, C., Moreci, P., Ryan, N., 1997. Schedule for affective disorders and schizophrenia for school-age children-present and lifetime version (K-SADS-PL): initial reliability and validity data. J. Am. Acad. Child Adolesc. Psychiatry 36 (7), 980–988.
Kessler, R.C., Berglund, P., Demler, O., Jin, R., Merikangas, K.R., Walters, E.E., 2005. Lifetime prevalence and age-of-onset distributions of DSM-IV disorders in the National Comorbidity Survey Replication. Arch. Gen. Psychiatry 62 (6), 593–602.
Kessler, R.C., Gruber, M., Hettema, J.M., Hwang, I., Sampson, N., Yonkers, K.A., 2008. Co-morbid major depression and generalized anxiety disorders in the National Comorbidity Survey follow-up. Psychol. Med. 38 (3), 365–374.
Kim, J.H., Hamlin, A.S., Richardson, R., 2009. Fear extinction across development: the involvement of the medial prefrontal cortex as assessed by temporary inactivation and immunohistochemistry. J. Neurosci. 29 (35), 10802–10808.
Kobayashi, K., Hsu, M., 2017. Neural mechanisms of updating under reducible and irreducible uncertainty. J. Neurosci. 37 (29), 6972–6982.
Koolschijn, P.C.M., Schel, M.A., de Rooij, M., Rombouts, S.A., Crone, E.A., 2011. A three-year longitudinal functional magnetic resonance imaging study of performance monitoring and test-retest reliability from childhood to early adulthood. J. Neurosci. 31 (11), 4204–4212.
Krain, A.L., Hefton, S., Pine, D.S., Ernst, M., Xavier Castellanos, F., Klein, R.G., Milham, M.P., 2006. An fMRI examination of developmental differences in the neural correlates of uncertainty and decision-making. J. Child Psychol. Psychiatry 47 (10), 1023–1030.
Krain, A.L., Gotimer, K., Hefton, S., Ernst, M., Castellanos, F.X., Pine, D.S., Milham, M.P., 2008. A functional magnetic resonance imaging investigation of uncertainty in adolescents with anxiety disorders. Biol. Psychiatry 63 (6), 563–568.
Lagattuta, K.H., Sayfan, L., 2011. Developmental changes in children's understanding of future likelihood and uncertainty. Cogn. Dev. 26 (4), 315–330.
LeDoux, J.E., Pine, D.S., 2016. Using neuroscience to help understand fear and anxiety: a two-system framework. Am. J. Psychiatr. 173 (11), 1083–1093.
Linton, S.R., Levita, L., 2021. Potentiated perceptual neural responses to learned threat during Pavlovian fear acquisition and extinction in adolescents. Dev. Sci. 24 (5), e13107.
Michalska, K.J., Feldman, J.S., Abend, R., Gold, A.L., Dildine, T.C., Palacios-Barrios, E.E., Atlas, L.Y., 2018. Anticipatory effects on perceived pain: associations with development and anxiety. Psychosom. Med. 80 (9), 853.
Michalska, K.J., Feldman, J.S., Ivie, E.J., Shechner, T., Sequeira, S., Averbeck, B., Pine, D. S., 2019. Early-childhood social reticence predicts SCR-BOLD coupling during fear extinction recall in preadolescent youth. Dev.Cogn.Neurosci. 36, 100605.
Michalska, K.J., Zhou, E., Borelli, J.L., 2022. School-aged children with higher anxiety symptoms show greater correspondence between subjective negative emotions and autonomic arousal. J. Exp. Child Psychol. 221, 105451.
Monga, S., Birmaher, B., Chiappetta, L., Brent, D., Kaufman, J., Bridge, J., Cully, M., 2000. Screen for child anxiety-related emotional disorders (SCARED): convergent and divergent validity. DepressionAnxiety 12 (2), 85–91.
Monk, C.S., Nelson, E.E., McClure, E.B., Mogg, K., Bradley, B.P., Leibenluft, E., Pine, D.S., 2006. Ventrolateral prefrontal cortex activation and attentional bias in response to angry faces in adolescents with generalized anxiety disorder. Am. J. Psychiatr. 163 (6), 1091–1097.
Morris, J.S., Öhman, A., Dolan, R.J., 1998. Conscious and unconscious emotional learning in the human amygdala. Nature 393 (6684), 467–470.
Morriss, J., Christakou, A., Van Reekum, C.M., 2015. Intolerance of uncertainty predicts fear extinction in amygdala-ventromedial prefrontal cortical circuitry. Biol. Mood Anxiety Disord. 5 (1), 1–13.
Morriss, J., Christakou, A., Van Reekum, C.M., 2019a. Multimodal evidence for delayed threat extinction learning in adolescence and young adulthood. Sci. Rep. 9 (1), 1–10.
Morriss, J., Gell, M., van Reekum, C.M., 2019b. The uncertain brain: a co-ordinate based meta-analysis of the neural signatures supporting uncertainty during different contexts. Neurosci. Biobehav. Rev. 96, 241–249.
Morriss, J., Biagi, N., Dodd, H., 2020. Your guess is as good as mine: a registered report assessing physiological markers of fear and anxiety to the unknown in individuals with varying levels of intolerance of uncertainty. Int. J. Psychophysiol. 156, 93–104.
Morriss, J., Bell, T., Biagi, N., Johnstone, T., Van Reekum, C.M., 2021a. Intolerance of uncertainty is associated with heightened responding in the prefrontal cortex during cue-signaled uncertainty of threat. Cogn.Affect.Behav.Neurosci. 1–11.
Morriss, J., Bennett, K.P., Larson, C.L., 2021b. I told you it was safe: associations between intolerance of uncertainty and different parameters of uncertainty during instructed threat of shock. J. Behav. Ther. Exp. Psychiatry 70, 101620.
Morriss, J., Tupitsa, E., Dodd, H.F., Hirsch, C.R., 2022a. Uncertainty makes me emotional: uncertainty as an elicitor and modulator of emotional states. Front. Psychol. 13, 777025.
Morriss, J., Bradford, D.E., Wake, S., Biagi, N., Tanovic, E., Kaye, J.T., Joormann, J., 2022b. Intolerance of uncertainty and physiological responses during instructed uncertain threat: a multi-lab investigation. Biol. Psychol. 167, 108223.
Nelson, B.D., Hajcak, G., 2017. Anxiety and depression symptom dimensions demonstrate unique relationships with the startle reflex in anticipation of unpredictable threat in 8 to 14 year-old girls. J. Abnorm. Child Psychol. 45 (2), 397–410.
O'Doherty, J., Critchley, H., Deichmann, R., Dolan, R.J., 2003. Dissociating valence of outcome from behavioral control in human orbital and ventral prefrontal cortices. J. Neurosci. 23, 7931–7939.
Öhman, A., Mineka, S., 2001. Fears, phobias, and preparedness: toward an evolved module of fear and fear learning. Psychol. Rev. 108 (3), 483.
Osmanağaoğlu, N., Creswell, C., Dodd, H.F., 2018. Intolerance of uncertainty, anxiety, and worry in children and adolescents: a meta-analysis. J. Affect. Disord. 225, 80–90.
Palitz, S.A., Rifkin, L.S., Norris, L.A., Knepley, M., Fleischer, N.J., Steinberg, L., Kendall, P.C., 2019. But what will the results be?: learning to tolerate uncertainty is associated with treatment-produced gains. J.Anxiety Disord. 68, 102146.
Pattwell, S.S., Duhoux, S., Hartley, C.A., Johnson, D.C., Jing, D., Elliott, M.D., Lee, F.S., 2012. Altered fear learning across development in both mouse and human. Proc. Natl. Acad. Sci. 109 (40), 16318–16323.

Paulus, M.P., Stein, M.B., 2010. Interoception in anxiety and depression. Brain Struct. Funct. 214 (5), 451–463.
Payzan-LeNestour, E., Bossaerts, P., 2011. Risk, unexpected uncertainty, and estimation uncertainty: Bayesian learning in unstable settings. PLoS Comput. Biol. 7 (1), e1001048.
Radoman, M., Lieberman, L., Jimmy, J., Gorka, S.M., 2021. Shared and unique neural circuitry underlying temporally unpredictable threat and reward processing. Soc. Cogn. Affect. Neurosci. 16 (4), 370–382.
Rangel, A., Camerer, C., Montague, P.R., 2008. A framework for studying the neurobiology of value-based decision making. Nat. Rev. Neurosci. 9 (7), 545–556.
Rolls, E.T., 2000. The orbitofrontal cortex and reward. Cereb. Cortex 10 (3), 284–294.
Sarinopoulos, I., Grupe, D.W., Mackiewicz, K.L., Herrington, J.D., Lor, M., Steege, E.E., Nitschke, J.B., 2010. Uncertainty during anticipation modulates neural responses to aversion in human insula and amygdala. Cereb. Cortex 20 (4), 929–940.
Schienle, A., Köchel, A., Ebner, F., Reishofer, G., Schäfer, A., 2010. Neural correlates of intolerance of uncertainty. Neurosci. Lett. 479 (3), 272–276.
Schmitz, A., Merikangas, K., Swendsen, H., Cui, L., Heaton, L., Grillon, C., 2011. Measuring anxious responses to predictable and unpredictable threat in children and adolescents. J. Exp. Child Psychol. 110 (2), 159–170.
Schoenbaum, G., Roesch, M., 2005. Orbitofrontal cortex, associative learning, and expectancies. Neuron 47 (5), 633–636.
Shankman, S.A., Gorka, S.M., Nelson, B.D., Fitzgerald, D.A., Phan, K.L., O'Daly, O., 2014. Anterior insula responds to temporally unpredictable aversiveness: an fMRI study. Neuroreport 25 (8), 596.
Shiba, Y., Santangelo, A.M., Roberts, A.C., 2016. Beyond the medial regions of prefrontal cortex in the regulation of fear and anxiety. Front. Syst. Neurosci. 10, 12.
Simmons, A., Matthews, S.C., Paulus, M.P., Stein, M.B., 2008. Intolerance of uncertainty correlates with insula activation during affective ambiguity. Neurosci. Lett. 430 (2), 92–97.
Smith, A.R., White, L.K., Leibenluft, E., McGlade, A.L., Heckelman, A.C., Haller, S.P., Pine, D.S., 2020. The heterogeneity of anxious phenotypes: neural responses to errors in treatment-seeking anxious and behaviorally inhibited youths. J. Am. Acad. Child Adolesc. Psychiatry 59 (6), 759–769.
Somerville, L.H., Wagner, D.D., Wig, G.S., Moran, J.M., Whalen, P.J., Kelley, W.M., 2013. Interactions between transient and sustained neural signals support the generation and regulation of anxious emotion. Cereb. Cortex 23 (1), 49–60.
Taschereau-Dumouchel, V., Michel, M., Lau, H., Hofmann, S.G., LeDoux, J.E., 2022. Putting the "mental" back in "mental disorders": a perspective from research on fear and anxiety. Mol. Psychiatry 1–9.
Tanovic, E., Pruessner, L., Joormann, J., 2018. Attention and anticipation in response to varying levels of uncertain threat: an ERP study. Cogn.Affect.Behav.Neurosci. 18 (6), 1207–1220.
Tottenham, N., Tanaka, J.W., Leon, A.C., McCarry, T., Nurse, M., Hare, T.A., Nelson, C., 2009. The NimStim set of facial expressions: judgments from untrained research participants. Psychiatry Res. 168 (3), 242–249.
Wechsler, D., 1999. Wechsler Abbreviated Scale of Intelligence. The Psychological Corporation, San Antonio (TX).
Williams, L.E., Oler, J.A., Fox, A.S., McFarlin, D.R., Rogers, G.M., Jesson, M.A., Kalin, N. H., 2015. Fear of the unknown: uncertain anticipation reveals amygdala alterations in childhood anxiety disorders. Neuropsychopharmacology 40 (6), 1428–1435.
Windmann, S., Kirsch, P., Mier, D., Stark, R., Walter, B., Güntürkün, O., Vaitl, D., 2006. On framing effects in decision making: linking lateral versus medial orbitofrontal cortex activation to choice outcome processing. J. Cogn. Neurosci. 18 (7), 1198–1211.
Wu, S., Sun, S., Camilleri, J.A., Eickhoff, S.B., Yu, R., 2021. Better the devil you know than the devil you don't: neural processing of risk and ambiguity. NeuroImage 236, 118109.